H_2^+ (20–100-keV) collisions with H: Dissociative and nondissociative capture and ionization and pure-H-target ionization

C. McGrath,[1] M. B. Shah,[1] P. C. E. McCartney,[1] and J. W. McConkey[2]
[1]*The School of Mathematics and Physics, Queen's University Belfast, Belfast BT7 1NN, United Kingdom*
[2]*School of Physical Sciences, University of Windsor, Windsor, Ontario, Canada N9B 3P4*
(Received 22 June 2001; revised manuscript received 7 August 2001; published 19 November 2001)

Collision of the molecular hydrogen ion, H_2^+ in the energy range 20–100 keV with a H target has been investigated. Production of one or two fast protons or hydrogen atoms formed from the projectile breakup was distinguished by use of a Si-barrier detector. Cross sections were determined by coincidence-counting techniques between the target ions (separated by time-of-flight analysis), electrons, and one or two fast product particles. Capture processes are shown to dominate at the lower energies whereas pure target ionization is demonstrated to be the most likely process at 90 keV and higher energies. Such data are of importance in the understanding of astrophysical and high-temperature laboratory plasmas.

DOI: 10.1103/PhysRevA.64.062712 PACS number(s): 34.70.+e, 82.30.Fi, 52.20.Hv

I. INTRODUCTION

There is on-going interest in the collisions involving atomic hydrogen and the molecular H_2^+ ion. This has been stimulated by both the fundamental nature of the collision and application to astrophysical, e.g., Black [1], and laboratory plasmas, notably supplementary heating by neutral-beam injection in fusion devices [2]. H_2^+ ions also play an important role in the chemistry of the interstellar medium [3].

The possible reaction paths in the H_2^+-H collision system are shown below, where underlining represents a fast particle. They are

$$\underline{H}_2^+ + H \rightarrow \underline{H}^+ + \underline{H} + H \quad (1)$$

involving pure breakup of the projectile,

$$\underline{H}_2^+ + H \rightarrow \underline{H}_2 + H^+ \quad (2)$$

$$\rightarrow \underline{H} + \underline{H} + H^+ \quad (3)$$

involving pure and dissociative capture,

$$\underline{H}_2^+ + H \rightarrow \underline{H}_2^+ + H^+ + e \quad (4)$$

$$\rightarrow \underline{H}^+ + \underline{H} + H^+ + e \quad (5)$$

involving target ionization with the projectile remaining intact or fragmenting, and

$$\underline{H}_2^+ + H \rightarrow \underline{H}^+ + \underline{H}^+ + H + e \quad (6)$$

$$\rightarrow \underline{H}^+ + \underline{H}^+ + H^+ + 2e \quad (7)$$

involving projectile ionization (leading to Coulomb explosion) with the target remaining intact or ionized.

We have considered this collision system in the energy range of 20–100 keV. The aim of this paper is to present the cross sections for these individual reaction paths. The only published work from other laboratories, in this energy range for the H_2^+-H collision system, is that of McClure [4], although only total fast-proton production channels (1), (5), (6), and (7) was measured, i.e., individual channels were not specified and nothing was said of the final state of the target. In a previous paper [5] we presented data for the individual channels (1), (5), (6), and (7) over the limited energy range 40–100 keV. Now we have extended this work to cover a wider energy range and also to present data on the important reactions (2), (3), and (4) that are expected to dominate over this range. Collision of H_2^+ on a purely molecular hydrogen target is also being investigated [6] and will be presented in due course.

II. EXPERIMENTAL APPROACH

Some aspects of the apparatus have been described elsewhere, [5,7] and so only a brief description will be given here. The H_2^+ beam from the accelerator was arranged to intersect (at right angles) a highly dissociated thermal-energy beam of hydrogen produced by a tungsten tube furnace in a separate differentially pumped chamber. Slow target ions and electrons produced were extracted using electrostatic grids and detected using channel electron multipliers. The different ion species were identified by their time-of-flight (TOF) to the detector. The H_2^+ beam was pulsed (200 ns pulse width with 10^5 Hz repetition rate) to provide the timing. A suitably delayed extraction pulse enabled optimum detection of the thermal $\underline{H}^+$ from H ionization and discrimination against superthermal $\underline{H}^+$ from $\underline{H}_2$ dissociative ionization. For a 70-keV H_2^+ incident on the target, the corresponding TOF spectra for the slow ions are shown in Fig. 1 for the furnace cool (1400 K) and furnace hot (2500 K). It can be seen that the increase in temperature produces the expected increase in the H^+ signal and the corresponding reduction in the H_2^+ signal.

The projectile products were separated into the different ion species and neutrals by the use of electrostatic-deflection plates after the interaction region. The H_2^+ main beam was monitored using a Faraday cup. Both the pressure and current monitors were routed through voltage-to-frequency con-

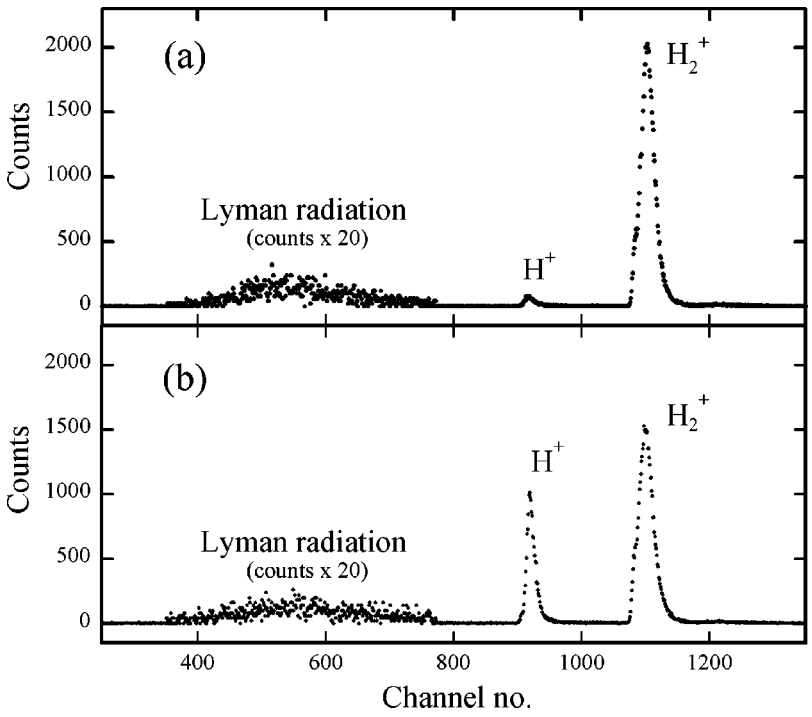

FIG. 1. Typical TOF spectra for slow target ions produced in the collision of 70-keV H_2^+ ions with the hydrogen target when the furnace is (a) cool (1400 K) and (b) hot (2500 K).

verters to minimize errors from these sources. The neutrals formed by electron capture or fragmentation of the H_2^+ ions were detected using a channeltron in the straight through position. Fast $\underline{H}^+$ fragments were deflected into a Si-barrier detector (Canberra PIPS PD100) that allowed discrimination between one or two fast-proton detection. Pulse height output from the solid-state detector clearly separates fast $1\underline{H}^+$ and $2\underline{H}^+$ production as shown in Fig. 2(a) for 70-keV incident H_2^+ ions.

A time window derived from the TOF spectra, corresponding to slow target products H^+ or H_2^+, was used to gate the output of the energy detector to obtain coincidence spectra, shown in Figs. 2(b) and 2(c), respectively. Then processes (5) and (7) can be determined by integrating the area under the $1\underline{H}^+$ peak and the $2\underline{H}^+$ peak in Fig. 2(b).

Signals for the capture channels (2) and (3) were obtained from TOF spectra such as in Fig. 1 but using appropriate timing derived from the fast neutral detector. Likewise, sig-

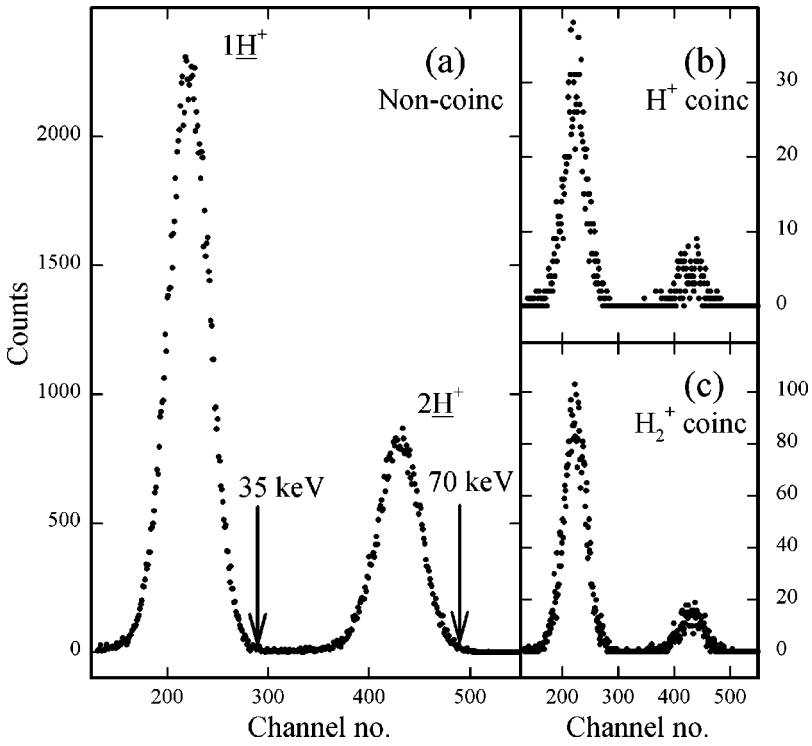

FIG. 2. Energy spectra obtained from the solid-state detector for 70-keV H_2^+ impact on H, distinguishing between the fast-projectile fragments, $1\underline{H}^+$ and $2\underline{H}^+$, for (a) noncoincidence mode and coincidence mode with (b) H^+ and (c) H_2^+ target products, respectively.

nals for the target ionization channels (4), (5), and (7) were also obtained from TOF spectra with the start pulse to the timing unit coming from electron detection.

The total coincidence signal for $\underline{H}^+$ formed in production with a charged target species, per unit primary ion current, measured with the furnace at temperature T (2500 K), is given by

$$S^T_{H^+} = S^T_{H^+}(H) + S^T_{H^+}(H_2) + S_B, \tag{8}$$

where $S^T_{H^+}(H)$ is the required signal, due to H_2^+ collisions with H atoms and $S^T_{H^+}(H_2)$ is the contribution from the undissociated H_2 in the crossed-beam region. The background contribution S_B arises from the dissociative ionization of residual gases (mainly H_2O) in the chamber and is measured in the absence of gas flow to the furnace.

To assess the molecular component in Eq. (8), the furnace was operated at a low temperature T_0 at which the target beam was entirely molecular. At this temperature, the total coincidence signal is given by

$$S^{T_0}_{H^+} = S^{T_0}_{H^+}(H_2) + S_B, \tag{9}$$

where $S^{T_0}_{H^+}(H_2)$ is the contribution from dissociative ionization of H_2 molecules. Using the procedure outlined in [8], the required signal in Eq. (8), $S^T_{H^+}(H)$, was calculated from which the individual cross sections were determined using

$$\sigma(H) = \frac{1}{k\mu} S^T_{H^+}(H), \tag{10}$$

where μ is the effective target thickness presented by the H atoms to the H_2^+ beam and k is a constant that reflects the efficiency of detection of the collision products.

It is important to note that for channels (1) and (6) no charged target products are available to provide unique identification through coincidence methods. For these, it was necessary to carry out measurements that only involved the fast projectile products, $1\underline{H}^+$ and $2\underline{H}^+$. For these noncoincidence measurements, the fragmentation of the H_2^+ ion can occur at any point along its path in the main chamber until projectile product separation in the electrostatic deflection field. H_2 diffusion out of the target beam into the surrounding region can provide a substantial contribution to the total fast product signal. This was taken into account by flooding this surrounding region with gas (carefully introduced via a remote needle valve) of pressure equal to that attained when the target beam was introduced.

A. Normalization procedures

In the recording of fast $1\underline{H}^+$ and $2\underline{H}^+$ products in coincidence with slow H^+ ions [corresponding to processes (5) and (7)] the data was normalized to the impact-ionization measurements of Shah and Gilbody [8] at 100 keV (with an uncertainty of $\pm 5\%$).

For measurements involving electrons, the coincidence signals between the electron detector and the slow-ion detector were normalized also to the 100-keV ionization measurements of Shah and Gilbody [8].

Capture channels were determined by coincidence counting between fast neutrals recorded by a channeltron placed in the straight-through position and the slow-target-ion detector. The coincidence signal was normalized through the use of H^+-H capture cross sections of McClure [9] at an impact energy of 30 keV (with an uncertainty of $\pm 5\%$).

To provide cross sections for the complete set of processes (1)–(7), noncoincidence measurements involving production of $1\underline{H}^+$ and $2\underline{H}^+$ fast ions were normalized to the total $\underline{H}^+$ production cross sections ($\pm 10\%$ uncertainty) of McClure [4].

B. Determination of individual cross sections

As noted above, cross sections for processes (5) and (7), σ_5 and σ_7, are obtained directly from the coincidence recording of fast $1\underline{H}^+$ and $2\underline{H}^+$ products with slow H^+ ions. From the coincidence measurements between the fast neutral products and the slow H^+, cross sections for the sum of processes (2), (3), and (5) were obtained. Subtraction of σ_5 then yielded the sum of the capture cross sections, $\sigma_{2,3}$. Likewise, the coincidence signal involving electrons and slow ions gave the sum of the cross sections for channels (4), (5), and (7). The cross section for channel (4), σ_4, was obtained by direct subtraction of σ_5 and σ_7. In the electron–slow-H^+ coincidence, process (7) would be detected with a higher efficiency than processes (4) and (5), because of the two electrons involved. Consequently, the value for σ_4 represents an upper bound, but it is worth noting that σ_7 is over an order of magnitude smaller than σ_4. The noncoincidence measurements of $1\underline{H}^+$ and $2\underline{H}^+$ corresponding to cross sections of the sum of processes (1) and (5) and (6) and (7), respectively, were obtained. Appropriate subtractions gave the cross sections σ_1 and σ_6.

The solid-state detector had a lower limit of 20 keV for $1\underline{H}^+$ detection, below which it was not possible to discriminate against thermal noise. The 20- and 30-keV data for channels (1) and (5) were obtained by replacing this detector with a channeltron. As a result of this, a small additional uncertainty arose in σ_1 and σ_5 because of the relatively small amounts that processes (6) and (7) contribute. The low-energy data were normalized to our values for σ_1 and σ_5 in an overlapping region at 40 keV.

III. RESULTS AND DISCUSSION

The cross sections for channels (1) to (7) in the energy range 20–100 keV are shown in Fig. 3 and tabulated in Table I. The error bars shown correspond to the statistical uncertainty and the reproducibility of the temperature/pressure settings affecting the H-atom number densities. Procedures used to extract the individual cross sections together with assigning absolute values to our raw data lead to additional uncertainties of $\pm 5\%$ for σ_5 and σ_7, $\pm 8\%$ for $\sigma_{2,3}$, $\pm 11\%$ for σ_1 and σ_6, and $\pm 7\%$ for σ_4.

As can be seen in Fig. 3, the electron-capture cross section, $\sigma_{2,3}$, dominates at the lower energies. We were not

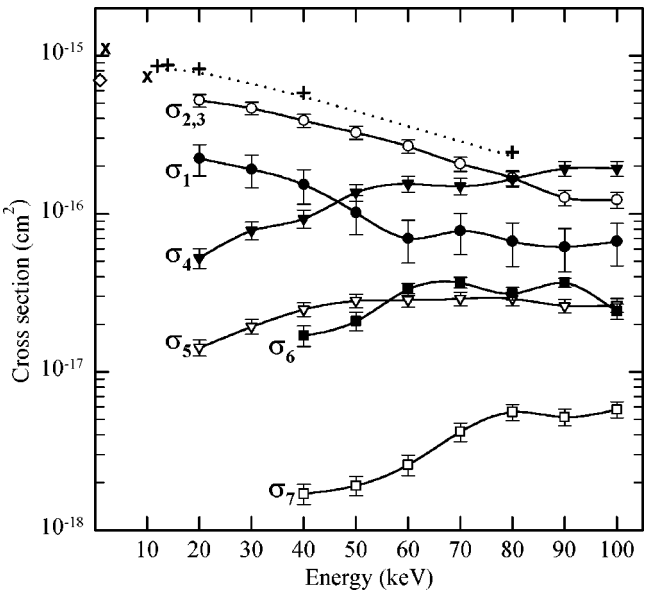

FIG. 3. Measured cross sections for the processes that occur for the H_2^+-H collision system in the energy range 20–100 keV (present and Ref. [6]); +, detailed balance calculations based on Barnett [11]; ×, Fite *et al.* [12]; and ◇, Campbell *et al.* [13]. Error bars do not include contribution from normalization procedures (see text). Barnett [11] and Fite *et al.* [12] data are subject to 30% accuracy.

able, however, to separate the production of 2H and H_2. This could have been achieved by scanning a slit across the face of the fast detector [10], but was not feasible in this study. The dominant process at higher energies is channel (4), involving pure ionization of the target.

No other experimental or theoretical data are available for direct comparison with those shown in Fig. 3. Fite *et al.* [12] have measured the electron-capture channel (2) over the energy range 100–10 000 eV. Unfortunately, these do not overlap with our data, but as can be seen from Fig. 3, the two data sets are certainly not inconsistent with one another. Their data indicate that the cross section for channel (2) goes through a maximum at 2 keV and drops off quite quickly as the energy is increased. Interestingly, the data lie somewhat higher than the 1-keV datum point of Campbell *et al.* [13] for the parallel process where H_2 rather than H is used as the target. Naively, one might expect the cross section to be larger for the molecular target. The explanation probably lies in the normalization methods employed by the two experimental groups.

The remaining data set shown in Fig. 3 has been obtained by applying a detailed balancing procedure to data for the time-inverse reaction, $H^+ + H_2 \rightarrow H + H_2^+$ given in the compilation of Barnett [11]. We appreciate that there are limitations to the accuracy of this procedure, due mainly to a lack of detailed knowledge of the vibrational distributions of the molecular projectile ions and the state-to-state cross sections. However, it does provide a reasonable data set for comparison purposes and as can be seen they seem to form a consistent extension to the low-energy data of Fite *et al.* [12]. Also, the data lie parallel to and only slightly higher than our data. Since our data contain contributions from both processes (2) and (3), this excellent agreement seems to suggest that contributions from the dissociative-capture process (3) may be small. This is in accord with the energy-defect arguments, process (3) have an energy defect of 6.4 eV compared to 1.9 eV for process (2).

It is well known that electron-impact ion sources produce H_2^+ ions that can be highly vibrationally excited [14–16]. The state-prepared experimental work involving capture collisions below 1 keV of Campbell *et al.* [13] in H_2 and Latimer and Campbell [17] in Ar show that capture cross sections are highly dependent on the vibrational state only at very low energies and become insensitive by 1 keV. The excellent agreement between the time-inverse experiments noted above seem to suggest that vibrational state effects play a minor role at higher energies too. On the other hand, for collisions dominated by dissociative channels, the cross sections remain greatly influenced by the vibrational-state population at all energies, as shown by the 1-keV measurements of Lindsay *et al.* [18] for excitation collisions to the $2p\sigma_u$ state in H_2, and the high-energy Born calculations of Peek [19] in H.

Our H_2^+ vibrational distribution is most likely determined by Franck-Condon effects in our low-pressure ion source [14], and hence is known at least approximately. Despite this lack of definition, the data is still very relevant to a tokamak

TABLE I. Measured cross sections for the processes that occur for the H_2^+-H collision system in the energy range 20–100 keV. Errors do not include those due to normalization procedures (see text).

Energy (keV)	Cross sections ($\times 10^{-16}$ m^2)					
	σ_1	$\sigma_{2,3}$	σ_4	σ_5	σ_6	σ_7
20	2.2±0.5	5.2±0.5	0.53±0.08	0.14±0.02		
30	1.9±0.5	4.7±0.4	0.79±0.10	0.19±0.03		
40	1.5±0.4	3.9±0.4	0.93±0.12	0.25±0.03	0.17±0.04	0.017±0.003
50	1.0±0.3	3.3±0.3	1.37±0.16	0.28±0.03	0.21±0.05	0.019±0.003
60	0.70±0.21	2.7±0.3	1.55±0.18	0.29±0.03	0.33±0.08	0.026±0.004
70	0.78±0.23	2.1±0.2	1.50±0.17	0.29±0.03	0.37±0.09	0.042±0.006
80	0.67±0.21	1.69±0.18	1.66±0.17	0.29±0.03	0.31±0.08	0.056±0.007
90	0.62±0.19	1.27±0.14	1.94±0.21	0.26±0.03	0.37±0.09	0.052±0.006
100	0.67±0.20	1.23±0.14	1.94±0.21	0.26±0.03	0.24±0.06	0.058±0.007

and stellarator neutral-beam injection systems [2] where a similar population distribution will occur.

The other processes shown in Fig. 3 involve the breakup of the projectile with the possibility of further ionization of the projectile and/or target. These have been discussed previously [5] and so no further comments will be made except to point out that the new lower-energy data are natural extensions of the previous trends.

ACKNOWLEDGMENTS

The authors wish to acknowledge financial assistance from the U.K. EPSRC and the Neutral Beam Injection group at the Max Planck Institute [2]. J.W.M. thanks NSERC, Canada for financial support. C.M. is indebted to the Department of Education, Northern Ireland for financial help. We thank Jim McGuire and Bert van Zyl for helpful insights.

[1] J.H. Black, Faraday Discuss. **109**, 257 (1998).
[2] W. Ott, D. Hartmann, F.P. Penningsfeld, and E. Speth, *Proceeding of the 27th EPS Conference on Controlled Fusion and Plasma Physics*, edited by K. Szego, T.N. Todd, and S. Zoletnik (EPS, Budapest, 2000), Vol. 24B, p. 1617.
[3] W.D. Watson, in *Atomic & Molecular Physics and the Interstellar Matter*, edited by R. Balian, P. Encrenaz, and J. Lequeux (North-Holland, Amsterdam, 1995).
[4] G.W. McClure, Phys. Rev. **153**, 182 (1967).
[5] P.C.E. McCartney *et al.*, J. Phys. B **32**, 5103 (1999).
[6] C. McGrath *et al.*, *Proceedings of CAARI XVI*, edited by J.L. Duggan and J.L. Morgan (University of North Texas, Denton, 2000).
[7] M.B. Shah, D.S. Elliot, and H.B. Gilbody, J. Phys. B **20**, 3501 (1987).
[8] M.B. Shah and H.B. Gilbody, J. Phys. B **14**, 2361 (1981).
[9] G.W. McClure, Phys. Rev. **148**, 47 (1966).
[10] G.W. McClure, Phys. Rev. **130**, 1852 (1963).
[11] C. F. Barnett, ONRL Report No. 6086, 1990 (unpublished).
[12] W.L. Fite, R.T. Blackman, and W.R. Snow, Phys. Rev. **112**, 1161 (1958).
[13] F.M. Campbell, R. Browning, and C.J. Latimer, J. Phys. B **14**, 3493 (1981).
[14] G.H. Dunn and B. Van Zyl, Phys. Rev. **154**, 40 (1967).
[15] B. Peart and K.T. Dolder, J. Phys. B **5**, 860 (1972).
[16] F. von Busch and G.H. Dunn, Phys. Rev. A **5**, 1762 (1972).
[17] C.J. Latimer and F.M. Campbell, J. Phys. B **15**, 1765 (1982).
[18] B.G. Lindsay, F.B. Yousif, and C.J. Latimer, J. Phys. B **21**, 2593 (1988).
[19] J.M. Peek, Phys. Rev. **140**, A11 (1965).